An Overview on Mathematical Models of Human Crystalline Lens

S. Talu[1], S. Giovanzana[2], S.D. Talu[3], and M. Talu[4]

[1] Faculty of Mechanics / Department of Descriptive Geometry and Engineering Graphics, Technical University of Cluj-Napoca, Romania
[2] DAUR – Laboratory of Design Tools and Methods in Industrial Engineering, University of Padova, Padova 35100, Italy
[3] Faculty of Medicine / Department of Ophthalmology, "Iuliu Hatieganu" University of Medicine and Pharmacy Cluj-Napoca, Romania
[4] Faculty of Mechanics / Department of Applied Mechanics, University of Craiova, Romania

Abstract— **To describe the human crystalline lens, mathematical models are required. Advanced mathematical models are applied for human vision studies and biomechanical behavior of the crystalline lens. The accurate modeling of the crystalline lens is important in the development of intraocular lenses. This paper presents an overview of researches for human crystalline lens modeling using mathematical models.**

Keywords— **human visual system, lens geometry, computational lens models.**

I. Introduction

The human lens is an elastic capsule containing cellular tissue of non-uniform gradient index. This index is difficult to measure and makes it difficult to deal with human lens parameters, especially for posterior surface of the lens that is difficult to image since it is seen through all the previous layers. The lens grows continually throughout life, with new epithelial cells forming at the equator, all the properties of the lens, are then age-dependent.

The first one to use spherical curve to describe the lens shape was Gullstrand [1] in his eye model but from the first experimental data [2] it was seen that an aspherical coefficient must be taken into account also for the optical zones of the lens that are about 5 mm diameter for anterior surface and 4 mm diameter for posterior surface.

In Table 1 some experimental results for anterior and posterior human crystalline lens radii and asphericity are given, the earlier experiments present average data, instead more recent experiments are age-dependent.

Moreover it must be underlined that modern imaging techniques, e.g. magnetic resonance [3, 4], are able to produce 3D image of the lens against previous imaging techniques, e.g. Scheimpflug lamp [5], which are able to produce one single meridian image.

The accurate modeling of the crystalline lens is important in research of intraocular lenses, so mathematical models of the lens based on geometrical constraints derived by the images must be used.

In this paper an overview of the most known mathematical models used for modeling the human crystalline lens is presented and analyzed.

Table 1 Radii of curvature, conic asphericities and relevant standard deviations of anterior and posterior lens experimentally determined by various authors. Number of eye and age with related ranges or standard deviation are also reported (D stands for accommodation power in dioptres, A stands for age in years)

Author	Anterior radius (mm)	Anterior asphericity	Posterior radius (mm)	Posterior asphericity
Lowe and Clark (1973), in vivo	11.26	—	—	—
Howcroft and Parker (1977), in vitro	7.3 ± 0.3	– 1.08 ± 9.412	– 5.4 ± 0.1	– 0.12 ± 1.74
Glasser and Campbell (1999), in vitro	4.32 + 0.068·A	– 1	– 3.14 – 0.05·A	– 1
Dubbelman et al. (2001), slit lamp	12.9–0.057·A	– 4 ± 4.7	– 6.5 - 0.017·A	– 3 ± 3.6
Rosen et al. (2006), in vitro	7.5 + 0.046·A	– 0.8 ± 1.7	– 5.5	– 1.1 ± 1.5

In chapter II six different models are presented: conic model, figuring conicoid model, Hermans conic patch model, Kasprzak hyperbolic cosine model, Urs 10th–order Fourier series model, Giovanzana parametric model.

In chapter III are presented the results for curvature and longitudinal spherical aberration analysis for each model.

II. Materials and Methods

In this part six different mathematical models used to describe the lens shape are presented. All the models are rotationally symmetric along the optical axis z, and their form is presented in the yz-plane where y is the distance from the optical axis and z is the sagitta.

All the models presented in the following part will refer to Fig. 1 for the definition of geometrical constraints.

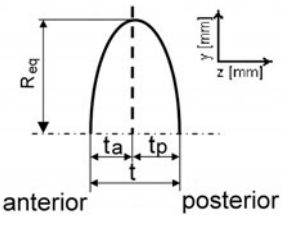

Fig. 1 Reference frame definition for a crystalline human lens

S. Vlad and R.V. Ciupa (Eds.): MEDITECH 2011, IFMBE Proceedings 36, pp. 240 – 245, 2011.
www.springerlink.com

A. *Conic Model*

The most known and used model for describing an optics revolution surface, e.g. cornea, crystalline lens and also ophthalmic lens, is the conic model. Its general equation is:

$$y^2 = 2Rz - (1 + q)\cdot z^2 \quad (1)$$

where R is radius of curvature and q is the aspheric coefficient. This formula is really important in optometry since the radius of curvature could be linked to the power of the surface described by equation (1). To derive these two coefficients a least square method is usually adopted to minimize the distance between the model and the raw points extracted by the imaging of the lens.

To describe the lens surface equation (1) must be modified adding two constraints, one for anterior and one for posterior part of the lens. These constraints are the anterior thickness t_a, and the posterior thickness t_p.

These geometrical constraints are derived from the image of the lens if the equator is clearly visible in the image, or are taken as a ratio of the total thickness, t, of the lens.

The final form of the conic model for anterior and posterior part of the lens in term of sagittal z is then:

$$y^2 = 2R_a\cdot(z + t_a) - (1 + q_a)\cdot(z + t_a)^2 \quad (2a)$$

$$y^2 = 2R_p\cdot(z - t_p) - (1 + q_p)\cdot(z - t_p)^2 \quad (2b)$$

where R_a is taken positive and R_p is taken negative; the form used in equation (2a) and (2b) let the lens equator stands on the y-axis.

B. *Figuring Conicoid Model*

The conic model itself does not provide a smooth junction of anterior and posterior part at the equator. This happens only for particular combinations of R and q.

To overcome this problem the figuring conicoid model is introduced [6]. The addition of figuring terms to equation (1) was already used in lens design [7] to modify the lens out of the optic zone.

In Smith's original formulation the number of figuring terms is not specified in a following work [8] the same work group define a number of three figuring conicoid, two of them linked to the geometry of the lens and one taken as free parameters assessed with least square method.

The final form of the figuring conicoid model for anterior and posterior part of the lens in term of sagittal z is then:

$$y^2 = 2R_a\cdot(z + t_a) - (1 + q_a)\cdot(z + t_a)^2 + \\ + v_{1a}\cdot(z + t_a)^3 + v_{2a}\cdot(z + t_a)^4 + v_{3a}\cdot(z + t_a)^5 \quad (3a)$$

$$y^2 = 2R_p\cdot(z - t_p) - (1 + q_p)\cdot(z - t_p)^2 + \\ + v_{1p}\cdot(z - t_p)^3 + v_{2p}\cdot(z - t_p)^4 + v_{3p}\cdot(z - t_p)^5 \quad (3b)$$

where v_{1a}, v_{2a} and v_{3a} are the figuring terms for anterior part and v_{1p}, v_{2p} and v_{3p} are the figuring terms for posterior part. Three conditions must be satisfied at the equator of coordinate $(0, R_{eq})$:

1. y at the equator must be the same for equation (3a) and (3b)
2. to have a smooth joint at the equator $dy/dz = 0$ when $z = 0$
3. to have a smooth joint at the equator also $(d^2y/dz^2)_a = (d^2y/dz^2)_p$

Solving these conditions for the equation (3a) and (3b) lead to the following equations for five parameters:

$$v_{1a} = (4R_{eq}^2 + 2q_at_a^2 + v_{3a}t_a^5 + 2t_a^2 - 6R_at_a)/t_a^3 \quad (4)$$

$$v_{2a} = -(3R_{eq}^2 + q_at_a^2 + 2v_{3a}t_a^5 + t_a^2 - 4R_at_a)/t_a^4 \quad (5)$$

$$v_{1p} = -(4R_{eq}^2 + 2q_pt_p^2 - v_{3p}t_p^5 + 2t_p^2 + 6R_pt_p)/t_p^3 \quad (6)$$

$$v_{2p} = -(3R_{eq}^2 + q_pt_p^2 - 2v_{3p}t_p^5 + t_p^2 + 4R_pt_p)/t_p^4 \quad (7)$$

$$v_{3p} = (q_p - q_a + 3v_{1p}(2t_p - t_a) + 6v_{2p}(2t_p - t_a)^2 - \\ - 3v_{1a}t_a - 6v_{2a}t_a^2 - 10v_{3a}t_a^3)/(10(2t_p - t_a)^3) \quad (8)$$

as it can be seen the free parameter v_{3a} can be found using a least square method.

C. *Hermans Conic Patch Model*

Another approach used by Hermans et al. [4] and based on the works of Dubbleman and Van der Heijde [5] and Hermans et al. [9], is to use different conic patches for the different zones of the lens. Their model is a parametric curve with a set of parameters that have a physical meaning; being formed by an anterior and posterior conic function as:

$$y^2 = 2R_a\cdot(z + t_a) \quad (9a)$$

$$y^2 = 2R_a\cdot(z - t_p) \quad (9b)$$

where the anterior part (9a) stops when y = 2.5 mm (the radius of anterior optical zone) and the posterior one (9b) when y = 2 mm (the radius of posterior optical zone). These functions are then linked together by other two conics for anterior and posterior part that join at the equator plane, and are of the form:

$$y = R_{eq} - \frac{cz^2}{1 + \sqrt{1 - kc^2z^2}} \quad (10)$$

where R_{eq} is the equatorial radius of the lens, $k = 1 + q$ is the asphericity coefficient and c is the curvature of the conicoid junction.

To assure a continuous junction and a continuous derivative between the different conic patches c and k for anterior and posterior surface must satisfied the following equations:

$$c = \frac{R_{eq} - y_p}{z_p\left[\frac{(R_{eq} - y_p)y_p}{r} + z_p\right]} \quad (11)$$

$$k = \frac{z_p\left[\frac{2(R_{eq} - y_p)y_p}{r} + z_p\right]}{(R_{eq} - y_p)^2} \quad (12)$$

where the terms (z_p, y_p) stands for the interception of the junction zones with the anterior or posterior optic zone.

D. Kasprzak Hyperbolic Cosine Model

Only few authors try to use different equations to describe both the anterior and posterior lens surface by a unique function, such as Kasprzak [10] hyperbolic cosine functions, Urs et al. [11] 10th–order Fourier series.

Kasprzak model is particularly interesting since it has a continuous curvature profile. This model uses a function to describe shape of the lens, given in polar coordinates:

$$\rho(\theta) = \rho_a(\theta) + \rho_p(\theta) + t/2 \quad (13)$$

where $\rho(\theta)$ is the distance from the lens centre along the angle θ that varies from 0 to π. The function has anterior and posterior contribution given by:

$$\rho_a(\theta)=(a_a/2)\cdot[\cosh((\pi - \theta)b_a) - 1]\cdot[1 - \tanh(m(s_a - \theta))] \quad (14a)$$

$$\rho_p(\theta)=(a_p/2)\cdot[\cosh(\theta b_p) - 1]\cdot[1 + \tanh(m(s_p - \theta))] \quad (14b)$$

where a and b can be derived by the lens radius and thickness t and the hyperbolic tangent terms give an appropriate cut–off function that reduce the mutual influence of the anterior and posterior contribution. The coefficients m and s describe the slope and the shift of the hyperbolic tangent. But Kasprzak do not give a method to evaluate the coefficients expect least square method.

E. Urs 10th–Order Fourier Series Model

As for Kasprzak model the Urs one [11] uses trigonometric functions instead of conics.

The Fourier series in a general form is written as:

$$\rho(\theta) = \sum_{n=0}^{10}(b_n)\cos(n\theta) \quad (15)$$

where the anterior thickness is found when $\theta = \pi$, the posterior thickness for $\theta = 0$ and the equator for $\theta = \pi/2$.

A remarkable difference between the Urs model and the Kasprzak one is that she was able to assess the b_n coefficients and create then an age-dependent model so that equation (15) becomes:

$$\rho(\theta) = \sum_{n=0}^{10}(A_{n1} + A_{n2} \times \text{age})\cos(n\theta) \quad (16)$$

In Table 2 are given the results of Urs et al. [11] experiment with the values of the A_n parameters, valid in the age range from 20 to 69. Other studies from Schachar [12, 13] demonstrate that out of this range the trend of radius of curvature and thickness may be different from Urs et al.

Table 2 Fourier coefficients of the age-dependent Fourier model

Parameter	A_{n1}	A_{n2}
A_0	2.6466	$812.11\cdot10^{-5}$
A_1	0.2246	$170.62\cdot10^{-5}$
A_2	– 0.97938	$– 297.37\cdot10^{-5}$
A_3	0.010573	$– 34.901\cdot10^{-5}$
A_4	0.37993	$– 26.276\cdot10^{-5}$
A_5	– 0.032321	$1.6647\cdot10^{-5}$
A_6	– 0.16846	$69.192\cdot10^{-5}$
A_7	0.027934	$– 9.5571\cdot10^{-5}$
A_8	0.066522	$– 42.251\cdot10^{-5}$
A_9	– 0.014232	$1.7295\cdot10^{-5}$
A_{10}	– 0.021375	$18.638\cdot10^{-5}$

F. Giovanzana Parametric Model

A parametric model that is able to assess the coefficients according to geometrical and optical constraints is the model proposed by Giovanzana et al. [14] and then revised in [15]. This model is based on Chien et al. model [16] but with the addiction of such constraints the coefficients can be assessed without any numerical method, e.g. least square.

The anterior part of the lens can be described by parametric function for $\pi/2 < u < \pi$ as:

$$z_a(u) = (b_{0a} + b_{1a}(\pi - u)^2 + b_{2a}(\pi - u)^4)\cdot\cos(u) \quad (17a)$$

$$y_a(u) = a_a\cdot\sin(u) \quad (17b)$$

while the posterior part of the lens can be written for $0 < u < \pi/2$ as:

$$z_p(u) = (b_{0p} + b_{1p}u^2 + b_{2p}u^4)\cdot\cos(u) \quad (18a)$$

$$y_p(u) = a_p\cdot\sin(u) \quad (18b)$$

To derive the coefficients a_i and b_i, geometrical constraints was imposed adopting the following considerations:

1. y at the equator must be the same for equation (17b) and (18b)
2. in the optical axis the value of the equation (17a) must be equal to thickness of the anterior side t_a

3. in the optical axis the value of the equation (18a) must be equal to thickness of the posterior side t_p

Also the following optical constraints are considered:

4. in the optical axis the curvature radius of the anterior side R_a must be respected
5. in the optical axis the curvature radius of the posterior side R_p must be respected
6. 6th–order Taylor expansion series of equation (17a) must be equal to the 6th–order Taylor expansion series of equation (2a) of the conic model
7. to ensure continuity in the equatorial plane the same radius of curvature for both sides of the lens was imposed

In particular the constraint number 6 allow to entangle the aspheric coefficient, typical of conic model, into the parametric model. Solving these conditions for the equation (17) and (18) lead to the following equations for eight parameters:

$$a_a = a_p = R_{eq} \tag{19}$$

$$b_{0a} = t_a \text{ and } b_{0p} = t_p \tag{20}$$

$$b_{1a} = 1/2\cdot(t_a - R_{eq}^2/R_a) \text{ and } b_{1p} = 1/2\cdot(t_p + R_{eq}^2/R_p) \tag{21}$$

$$b_{2a} = 5/24\cdot t_a - 1/12\cdot R_{eq}^2/R_a - (1 + q_a)/8\cdot R_{eq}^4/R_a^3 \tag{22}$$

$$b_{2p} = b_{2a} + 2\cdot(\pi^2 + 8)/\pi^4\cdot(t_a - t_p) - 2R_{eq}^2/\pi^2\cdot(1/R_a + 1/R_p) \tag{23}$$

These set of constraints are linked to the contour extremis of the lens profile, by thickness t and equatorial radius R_{eq}; to optical properties of the central zone, by the radius of curvature R; to the whole optical zone, by the aspherical coefficient q; and let the model to have a continuous curvature along the whole profile.

G. Methods

To analyse these models data in Smith et al. [8] are used. In particular are used as reference data of Kasprzak model since as already said the author don't give any method to find the model coefficients. Geometrical and optical constraints of the lens are summarised in Table 3. In particular in [8] the values of the asphericity coefficient q are not provided and are then founded with a least square method.

Table 3 Lens constraints

R_a	q_a	R_p	q_p	t	t_a / t_p	R_{eq}
5.431	– 0.078	– 4.454	– 0.61	5.014	0.874	3.992

Curvature analysis is performed on the different models. The radius of curvature is given by next formula:

$$R = \frac{\left((z_u)^2 + (y_u)^2\right)^{3/2}}{z_u y_{uu} - z_{uu} y_u} \tag{24}$$

where R is the radius of curvature and y and z are parameterised respect to u.

III. Results

Using the data of Table 3 the conic model can be found. Applying formula (24) the curvature data is found and plotted against the distance from the optical axis (Fig. 2).

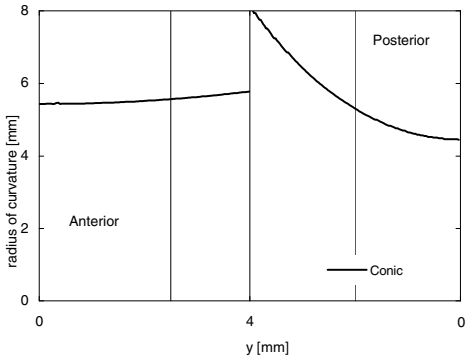

Fig. 2 Radius of curvature of the conic model versus y direction

Anterior part of the lens is on the left side from 0 to 4, and posterior one is on the right part from 4 to 0. The vertical lines in the plot represents from left to right the anterior optic zone, the equator, the posterior optic zone.

Both side of the lens present an increasing value or the radius of curvature according to the asphericity value.

It can be also seen the jump in curvature at the equator.

The figuring conicoid model parameters data are summarised in Table 4. In particular the value of parameter v_{3a} is found with a least square method, the rest of parameters are found according to formula in section II.B.

Table 4 Figuring conicoid model parameters

Parameter	Anterior surface	Posterior surface
q	– 0.078	– 0.61
v_1 (mm^{-1})	– 0.432650	0.179712
v_2 (mm^{-1})	0.142355	0.000749
v_3 (mm^{-1})	– 0.045000	0.000934

In Fig. 3 the radius of curvature for the figuring conicoid model is plotted against the distance from the optical axis.

It can be immediately seen that curvature of the model is continuous and in both optic zones the curvature is close to the conic model.

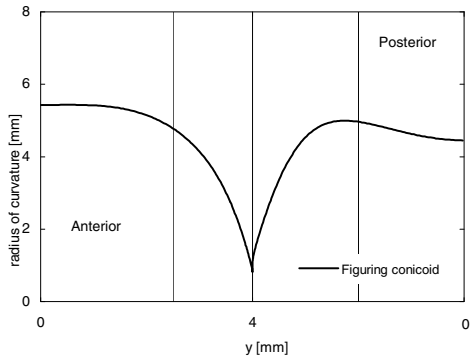

Fig. 3 Radius of curvature of the figuring conicoid model versus y direction

Hermans conic patch model parameters are summarised in Table 5. The parameters are concerning only the junction zones since both the optical zones have q = –1.

Table 5 Hermans model parameters

Parameter	Anterior surface	Posterior surface
c (mm^{-1})	0.786	0.672
k	0.309	0.245

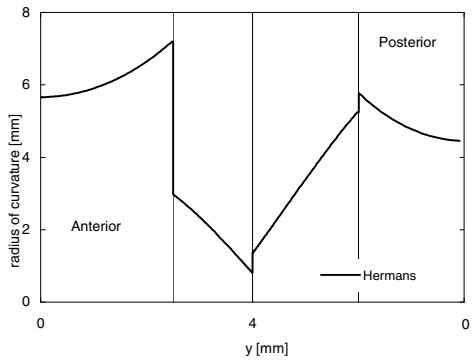

Fig. 4 Radius of curvature of the Hermans model versus y direction

In Fig. 4 the radius of curvature of the Hermans conic patch model is plotted. As it can be seen the curvature in the optical zones does not follow the conic model due to different asphericity coefficient. Moreover the model presents a curvature jump for every zone passage.

In Table 6 the data for Kasprzak model taken from [8] are summarised. All the coefficients are derived by least square method.

Table 6 Kasprzak model parameters

Parameter	Anterior surface	Posterior surface
a	0.965	0.977
b	1.186	1.061
s	1.808	1.669
m	3.706	

In Fig. 5 the radius of curvature for the Kasprzak model is plotted. It can be seen that this model presents a continuous curvature all along the lens shape.

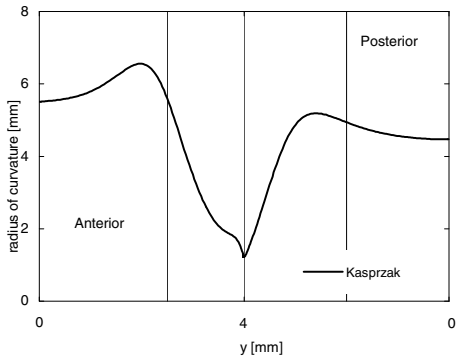

Fig. 5 Radius of curvature of the Kasprzak model versus y direction

Urs model depends only by age from [8] is known that the lens analysed is a seven year old ex vivo lens it is decided to take the age input data for Urs parameters as 7.

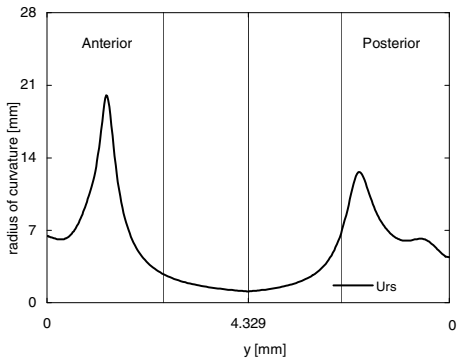

Fig. 6 Radius of curvature of the Urs model versus y direction

Radius of curvature for the Urs model is plotted in Fig. 6. As it can be seen the model presents much more variability against the other models.

In Table 7 the parameters for Giovanzana model are found using as input the data of Table 3.

Table 7 Giovanzana model parameters

Parameter	Anterior surface	Posterior surface
b_0	2.339	2.675
b_1	– 0.298	– 0.451
b_2	0.060	0.067

Fig. 7 presents the radius of curvature of Giovanzana model.

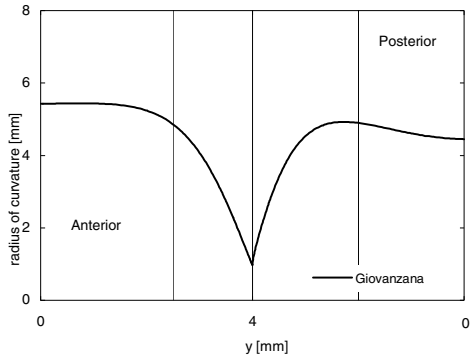

Fig. 7 Radius of curvature of the Giovanzana model versus y direction

As it can be seen the model is continuous all along the surface and is close to the conic model, in the optic zones, and to the figuring conicoid model all over the surface.

IV. Discussion and conclusion

Several simple models such as circular, parabolic or conic sections are usually adopted to describe the surfaces of the human crystalline lens.

More complex mathematical models such as figuring conicoid [8], conic patch [4], hyperbolic cosine [10], Fourier series [11], parametric curves [13] use more coefficients typically derived by fitting techniques [17], or derived from geometrical and optical constraints.

Figuring conicoid, Kasprzak, Urs and Giovanzana models present a continuous curvature that is important for models that can be used in FEM analysis.

Kasprzak and Urs models present more difficulties to assess the coefficients, the first one since is not given by the author any method to find them; the second since they are presented only dependent by age.

Figuring conicoid model and Giovanzana model are very similar in shape and in the way they assess the coefficients. However Giovanzana model is able to fully derive the coefficients by geometrical and optical constraints.

Both these models presents a radius of curvature similar to the conic model in the optical zone and this is for sure important for the optical properties of these two models that can be easily used then to modelised a human lens more similar to the real shape of the lens.

References

1. Gullstrand A (1909) Helmholz's handbuch der physiologichen optic, vol. 1, 3rd edition, english translation edited by Southall JP, 1924 Optical of America
2. Lowe R F, Clark B A (1973) Posterior corneal curvature. J Ophthalmlol 57: 464–470
3. Jones C E, Atchison D A, Meder R, Pope J M (2005) Refractive index distribution and optical properties of the isolated human lens measured using magnetic resonance imaging (MRI). Vision Res 45 (18): 2352–2366
4. Hermans E, Pouwels P J, Dubbelman M, Kuijer J P A, Van der Heijde R G L, Heethaar R M (2009) Constant volume of the human lens and decrease in surface area of the capsular bag during accommodation: an MRI and Scheimpflug study. Invest Ophth Vis Sci 50 (1): 281–289
5. Dubbelman M, Van der Heijde R G L (2001) The shape of the aging human lens: curvature, equivalent refractive index and the lens paradox. Vision Res 41: 1867–1877
6. Smith G (2003) The optical properties of the crystalline lens and their significance. Clin Exp Optom 86 (1): 3–18
7. Atchison D A (1992) Spectacle lens design: a review. Appl Opt 31 (19): 3579–3585
8. Smith G, Atchison D A, Iskander D R, Jones C E, Pope J M (2009) Mathematical models for describing the shape of the in vitro unstretched human crystalline lens. Vision Res 49: 2442–2452
9. Hermans E, Dubbleman M, Van der Heijde R G L, Heethaar R M (2007) The shape of the human lens nucleus with accommodation. J Vision 7 (10): 1–10
10. Kasprzak H T, Iskander D R (2006) Approximating ocular surfaces by generalised conic curves. Ophthal Physl Opt 26: 602–609
11. Urs R, Ho A, Manns F, Parel J (2010) Age–dependent Fourier model of the shape of the isolated ex vivo human crystalline lens. Vision Res 50: 1041–1047.
12. Schachar R A (2004) Central Surface Curvatures of Postmortem-Extracted Intact Human Crystalline Lenses. Ophthalmology 111 (9): 1699–1704
13. Schachar R A (2005) Growth patterns of fresh human crystalline lenses measured by in vitro photographic biometry. J Anat 206: 575–580
14. Giovanzana S, Savio G, Meneghello R, Concheri G (2011) Shape analysis of a parametric human lens model based on geometrical constraints. J Mod Opt: 1–11 DOI 10.1080/09500340.2011.554895
15. Giovanzana S (2011) A Virtual Environment for modeling and analysis of human eye. University of Padova
16. Chien M C, Tseng H, Schachar R A (2003) A mathematical expression for the human crystalline lens. Compr Ther 29: 245–258
17. Xirui Z, Yuhua P, Xiaobing W, Aizhen L (2008) Modeling of human crystalline lens. The 2nd Int. Conference on Bioinformatics and Biomedical Engineering (ICBBE 2008), Shanghai, China, pp. 1787–1791

Author: Stefan Talu
Institute: Faculty of Mechanics / Department of Descriptive Geometry and Engineering Graphics, Technical University of Cluj-Napoca
Street: B-dul Muncii Street no. 103-105
City: Cluj-Napoca
Country: Romania
Email: stefan_ta@yahoo.com